

Empirical Path Loss Prediction for Wireless Sensor Networks Operating in Sand and Dust Storms

Hana Mujlid*, Ivica Kostanic

Department of Electrical and Computer Engineering

ABSTRACT

This paper proposes an empirical model for prediction of the radio path loss in Wireless Sensor Networks (WSNs). The model applies to WSNs that are deployed in environments with dust and sand storms. It is developed as a result of statistical analysis of the measured data collected during dust and sand storms. The measured data were obtained at 2.4GHz and for different levels of the storm severity. The proposed model shows a very good agreement with the measured data. It is also demonstrated that the radio path loss correlates very well with the wind speed. Therefore, the wind may be considered as a principle source that determines the severity of the dust and sand storms from the path loss standpoint.

Keywords: Propagation loss, wireless sensor networks, sand storms.

Date of Submission: 12-01-2021

Date of Acceptance: 27-01-2021

I. INTRODUCTION

Wireless Sensor Networks (WSN) are deployed in all types of environments. They provide valuable environmental data that may be used for situation awareness, security, weather condition assessment, safety and many other purposes. The WSNs rely on radio communication to transfer the data between deployed WSN nodes. Since radio signal propagation is affected by the WSN surroundings, the deployment, operation and maintenance of a WSN depends a great deal on the environment where the network is deployed. There are several published studies [1-6] establishing that a radio signal in the presence of the dust storms encounters an increase of the propagation path loss. The effect is quite significant and it has a measurable impact on the operation of wireless systems [5, 6]. Therefore, in the process of wireless network planning, the potential of additional signal attenuation that is due to sand storms needs to be taken into account.

Most of the work published in the area of WSN deployment during the dust and sand storms documents measurement results. Beyond straightforward first order fit to measured data, a limited attention is placed on the statistical path loss modeling [5]. This paper attempts to provide a practical prediction model for estimation of the radio signal path loss within environments that are subject to sand and dust storms. The model is developed through statistical analysis of measured data. The data were collected in and around city of Al Kharj, Kingdom of Saudi Arabia and in 2.4GHz

ISM band. For the purpose of data collections, the authors have developed a custom measurements system that is described in great detail in the companion paper [6]. The 2.4GHz ISM band is the most popular frequency band for deployment of unlicensed wireless systems. It extends from 2400-2483.5MHz and it is used worldwide for deployment of WiFi (IEEE 802.11 b, g, n), Bluetooth, ZigBee (IEEE 802.15.4), and many other standard and proprietary technologies. This band is also one of the primary bands used for deployment of WSNs. These networks are typically deployed in the outdoor environment and therefore, they are exposed to the weather conditions. Also, they are deployed in configurations that are quite different than what is encountered in other wireless systems. Unlike, for example cellular systems, WSN are deployed using low power devices, with low antenna heights and with omnidirectional patterns. For such deployments, there is a general lack of relevant propagation models. This is especially true for the circumstances where besides terrain and manmade obstructions, the signal encounters additional impairments coming from the effects of the sand storms. The remaining of the paper is organized as follows. An overview of the measurement system implementation is presented in section II. A summary of measurement data campaign is presented in section III. The analytical form of the proposed propagation model is presented in section IV. The performance of the model is examined in section V. Finally, section VI summarizes findings and proposes some direction for future research.

II. SYSTEM DESCRIPTION

A block diagram of the measurement system is presented in Fig. 1 [6].

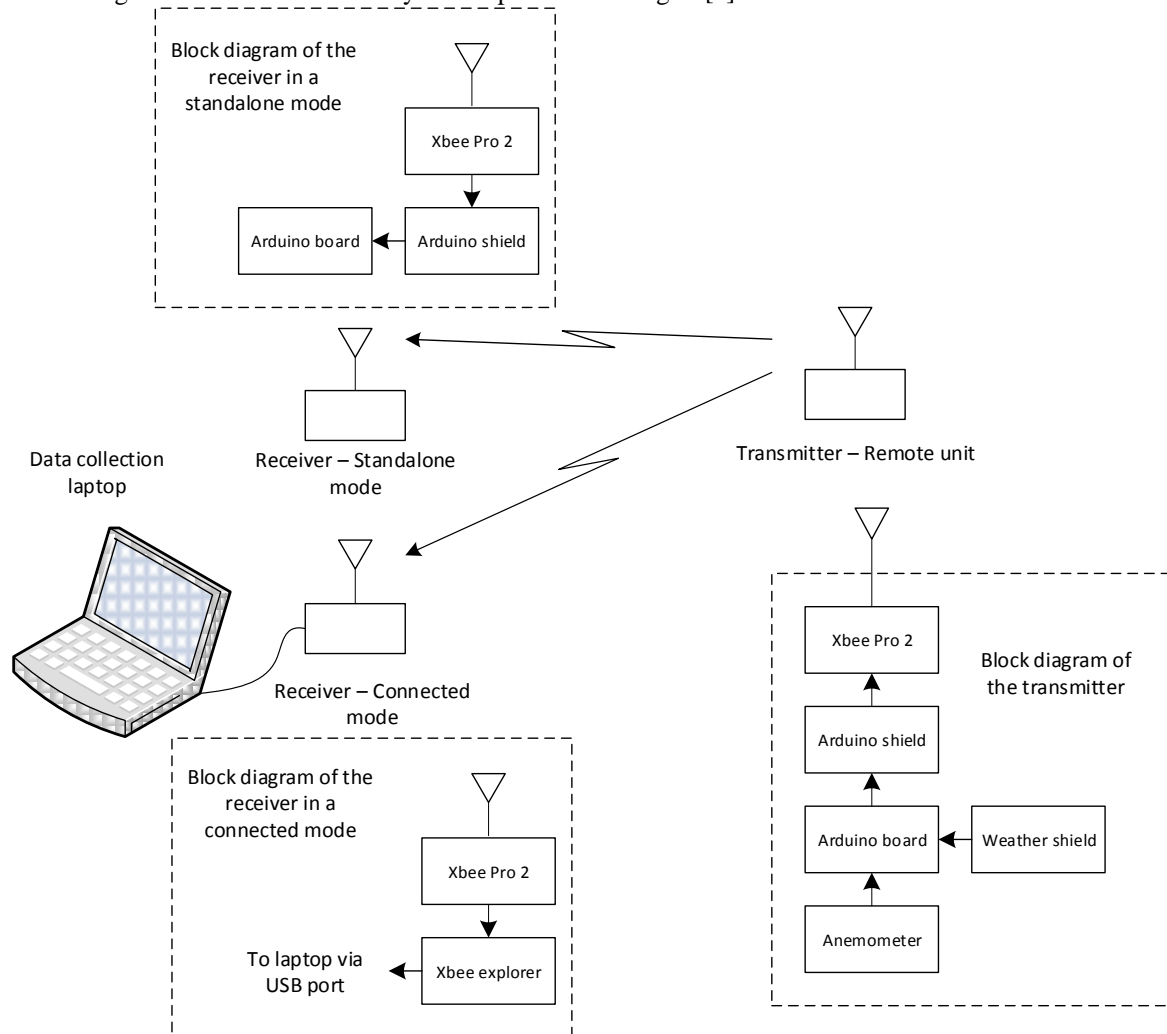


Figure 1: Block diagram of the measurement system

As seen, the system consists of three principal components.

1. *WSN transmitter.* The WSN transmitter consists of an Arduino board and with the Xbee PRO 2 radio [6]. The interface between the Arduino board and the Xbee transmitter is provided through

the Arduino shield. Additionally, the Arduino board at the transmitter is connected to a sensor board called Weather shield and to an external anemometer. The transmitter collects data as listed in Table 1.

TABLE 1. Measurements collected at the transmitter side

Measurement	Range
Temperature	22-59 °C
Pressure	500-1100 mbar
Humidity	0-100 %
Wind speed	0-82 kmph

The principle component for management of the transmitter is the Arduino board. The Arduino runs the software that collects the data from the Weather shield and the anemometer. The data

are then forwarded to Xbee PRO 2 radio and sent over to the receiver side. Unlike environmental parameters the Received Signal Level (RSL) measurement is performed by the Xbee receiver.

This measurement is used for estimation of the propagation path loss between the Xbee transmitter on the remote unit and the Xbee receiver at the base unit.

2. *WSN receiver.* The WSN receiver may operate in two different modes. The first mode is a *stand-alone mode*. In this mode, the receiver consists of an Arduino board, Arduino shield and Xbee PRO 2 radio. When the receiver is operating in a stand-alone mode, the data received by the Xbee radio are stored locally on a memory card that resides on the Arduino board. The stand-alone mode allows the system to operate in a severe sand storm, and it was used for most of the measurements. After the measurement session, the data stored on the memory card are uploaded onto the laptop for further processing.

Alternatively, the receiver may be configured to operate without the Arduino board. This mode is referred to as the *connected-mode*. In the connected mode, the Xbee radio is connected to a laptop through an interface board - Xbee explorer. In this mode, the data are stored directly to the laptop. When in connected mode, the user may monitor the data collection process on the laptop screen. However, this is only feasible in clear sky conditions.

3. *Collection laptop.* Collection laptop hosts software that is utilized for configuration of the measurement system and for the analysis of the data. Two software environments are used. Software X-CTU is used for configuring the Xbee radios and for formation of the WSN. The receiver Xbee radio is configured as the 802.15.4 network coordinator, while the transmitter unit is configured as a remote. The second software environment is the Arduino

board IDE. This software is used to program the Arduino board of the transmitter and the Arduino board of the receiver in the standalone mode. In the connected mode, the receiver does not use Arduino board and data are read directly from the Xbee receiver (Fig. 1).

III. MEASURED DATA

The measurements of the path loss are performed on a regular grid as presented in Fig 2. The receiver is placed in the center of the grid and the transmitter is moved between measurement points. The measurement points are placed on eight radials. The angle between the radials is 45 degrees. There are 5 measurement points at each radial. On a given radial, the measurement points are spaced 5 meters apart. The closest one is 5 meters from the receiver, and the furthest one is 25 meters away. Several hundreds of instantaneous path loss measurements are collected for each measurement point. The measurements at a single point are averaged to eliminate fast fading effects and yield one path loss measurement value. In a given experiment, a macroscopic (i.e. average) path loss value is obtained for each measurement point. Therefore, each experiment consists of 40 path loss measurements that were obtained across 8 different radials and 5 different radial distances.

Measured data are collected in four experiments. The experiments are defined on the basis of the sand storm severity. In the first experiment, the data are collected under a clear sky. This experiment is used as the baseline and it is referred to as E-1. The remaining three experiments are *dusty sky* (E-2), *sand storm* (E-3) and *heavy sand storm* (E-4) experiments.

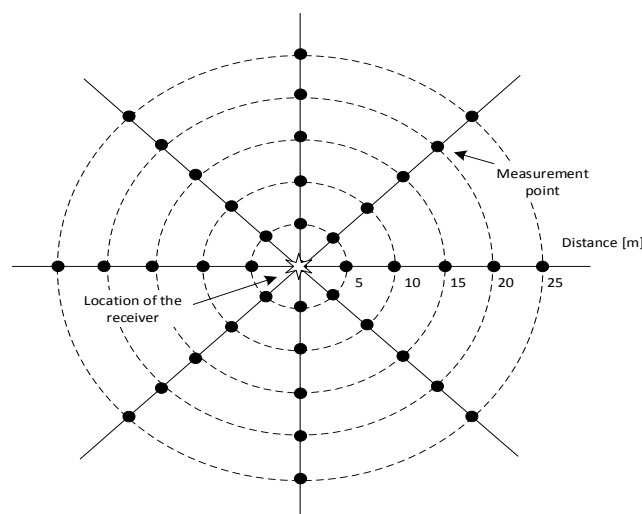


Figure 2: Location of the measurement points in data collection process

Detail report on collected data is provided in [6]. Tables 2 and 3 provide summary. Table 2 provides average path loss measurements, while Table 3 provides recorded environmental parameters associated with the four experiments. The path loss

measurements are averaged across all eight radials. This is justified on the basis of the uniformity of the environment. In all experiments, the environment was very similar along each of the eight radial directions.

TABLE 2. Average path loss as a function of distance for four experimental environments

TX-RX distance (m)	5	10	15	20	25
log(d/1m)	0.70	1.00	1.18	1.30	1.40
E1 – clear sky	74.64	83.34	90.32	92.77	93.07
E2 – dusty sky	76.24	84.63	92.85	94.87	98.66
E3 – sand storm	80.97	87.33	97.85	102.02	104.89
E4 – heavy sand storm	85.87	88.79	99.21	103.83	108.29

The most important environmental parameter that impacts the propagation is the wind speed. It is provided in the last column of Table 3 in both km/h and m/s. The wind lifts the particles of dust and sand into the air. It is reasonable to expect

that as the strength of the wind is increased, the density of the particles becomes higher and the impact on the propagation of the radio signals becomes more significant.

TABLE 3. Environmental parameters for four experiments

Environment	Humidity (%)	Temperature (C)	Pressure (mbar)	Wind speed (km/h, m/s)
E1 – clear sky	19.1	34.7	1060	2.3, 0.6
E2 – dusty sky	27.8	45.7	974	13, 3.6
E3 – sand storm	61.3	34.7	959	13.6, 3.8
E4 – heavy sand storm	49.0	36.1	984	26.3, 7.3

IV. PROPOSED PROPAGATION MODEL

The signal propagation scenario under consideration in this work is illustrated in Fig. 3. The scenario is seen as the extension of the basic two-ray propagation over flat reflective surface [7]. However, unlike the basic two ray propagation, the

scenario in Fig. 3 assumes that the space between the transmitter (TX) and the receiver (RX) contains a concentration of particles of dust or sand. These particles cause additional absorption of the energy of the radio signal and therefore, the propagation path loss is increased.

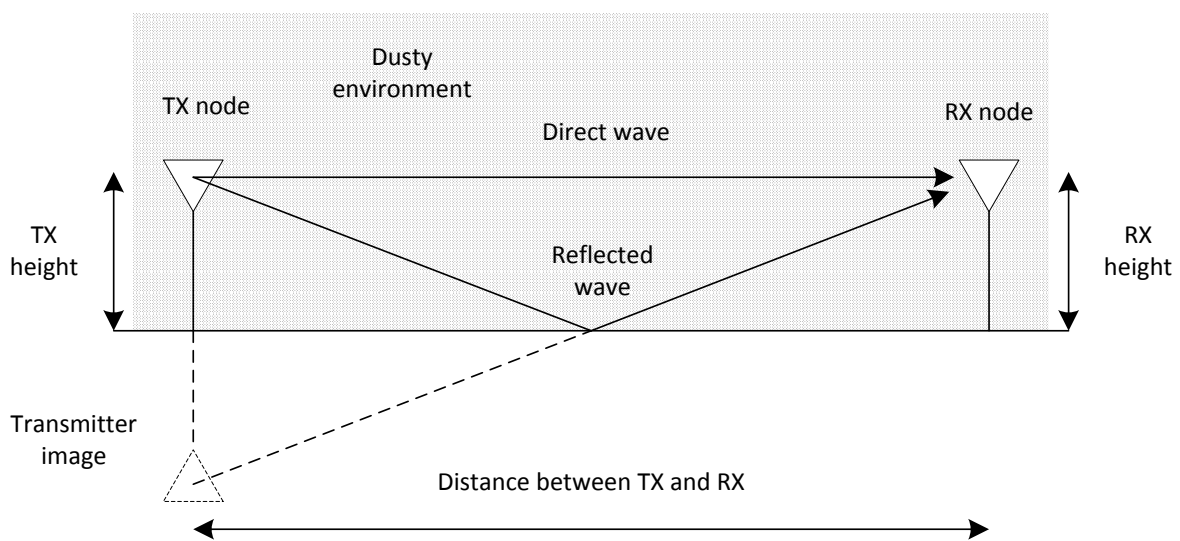


Figure 3: Geometry of radio signal propagation in presence of dust and sand

General form of the model equation

By following the same methodology as in [7] and taking into account the absorption from dust and send, one obtains the path loss in the form given by:

$$PL(d) = \frac{P_{TX}}{P_{RX}} = \underbrace{\left(\frac{4\pi d}{\lambda}\right)^2}_{\text{Two-ray part}} \underbrace{|1 + \rho \exp(-j\Delta\phi)|}_{\text{Absorption due to sand}} \underbrace{A(d)}_{\text{Absorption due to sand}} \quad (1)$$

Where, $PL(d)$ is the path loss between TX and RX that are separated by distance d , P_{TX} is the transmit effective radiated power, P_{RX} is the received power, λ is the wavelength of the propagating wave, ρ is the complex value of the reflecting coefficient of the ground and $\Delta\phi$ is the phase difference between the direct and reflected waves at the RX antenna that is due to the difference in the length of their propagation paths.

The term $A(d)$ represents the additional signal attenuation that is due to sand and dust absorption. Equation (1) assumes that both TX and RX antenna have unit gains.

From the geometry of the propagation scenario, presented in Fig. 3, one may easily obtain the value of the $\Delta\phi$ as:

$$\Delta\phi = \frac{\Delta d}{\lambda} \cdot 2\pi \quad (2)$$

where

$$\Delta d = d \left\{ \sqrt{1 + \frac{(h_{TX} + h_{RX})^2}{d^2}} - \sqrt{1 + \frac{(h_{TX} - h_{RX})^2}{d^2}} \right\} \quad (3)$$

In (3), quantities h_{TX} and h_{RX} represent the height of the transmitter and receiver antenna respectively. A significant factor in (1) is the reflection coefficient ρ . This factor depends on the properties of the ground and based on the ITU report published in [8], it may be determined using:

$$\rho = \frac{\sin(\varphi) - \sqrt{C}}{\sin(\varphi) + \sqrt{C}} \quad (4)$$

Where φ is the grazing angle given by:

$$\varphi = \tan^{-1}\left(\frac{h_{TX} + h_{RX}}{d}\right)$$

And

$$C = \eta - \cos^2(\varphi) \quad \text{for horizontal polarization} \quad (5)$$

$$C = (\eta - \cos^2(\varphi)) / \eta^2 \quad \text{for vertical polarization} \quad (6)$$

With

$$\eta = \epsilon_r(f) - j60\lambda\sigma(f) \quad (7)$$

Where

$\epsilon_r(f)$ relative permittivity of the ground surface at frequency f

$\sigma(f)$ conductivity (S/m) of the surface at frequency f

As seen in (2)-(7), at a given frequency, the reflection coefficient is a function of geometry, wave polarization and properties of the ground. More specifically, the reflection coefficient depends on the relative permittivity and conductivity of the ground. For the environments considered in this report, the relative permittivity is approximately 4.5 and the conductivity is 0.17 S/m, which are values typical for sand environments.

Term $A(d)$ in (1) captures additional loss that is due to presence of dust and sand. The model assume that this term is in the form that satisfies:

$$10 \log [A(d)] = 10\alpha \sqrt{\log\left(\frac{d}{1m}\right)} \quad (8)$$

Using (1) and (8), the path loss prediction of the model expressed in dB may be obtained as:

$$PL_{dB}(d) = 10 \log \frac{P_{TX}}{P_{RX}} = 20 \log \left(\frac{4\pi d}{\lambda}\right) - 20 \log |1 + \rho \exp(-j\Delta\phi)| + 10\alpha \sqrt{\log\left(\frac{d}{1m}\right)} \quad (9)$$

The model equation expressed in (9) has one parameter α , that is a property of the propagation environment. This parameter captures the magnitude of the additional attenuation that is due to the presence of the sand. The value of the parameter may be obtained from measured data. Using measurements reported in Table 2, numerical values for the experimental setup shown in Table 4, and the process of linear regression, the values of the parameter α for four different environments are obtained and reported in Table 5.

TABLE 4. Parameters of the experimental setup [6]

Parameter of the experimental setup	Symbol	Value	Unit
Height of the TX antenna	h_{TX}	0.1	meter
Height of the RX antenna	h_{RX}	0.1	meter

Relative permittivity of the ground	ϵ_r	4.5	N/A
Conductivity of the ground	σ	0.17	S/m
Frequency	f	2450	MHz

TABLE 5. Value of parameter α obtained through linear regression of the experimental data

Environment	α (dB)
E1 – clear sky	2.22
E2 – dusty sky	2.46
E3 – sand storm	2.95
E4 – heavy sand storm	3.21

Relationship between α and wind speed

It is reasonable to assume that the environmental parameter α in (9) is related to the concentration of the sand in the air. At the same time, the amount of the sand that is being lifted up during a sand storm is also related to the speed of the wind. Therefore, it is reasonable to expect that there is a dependence of α on the wind speed. For the data analyzed in this study, this dependence is illustrated in Fig. 4. The figure also shows a regression line and an equation that may be used for prediction of α on the basis of the known wind speed given in m/s. In other words, if the wind

speed in an area is available, the value of environmental parameter α may be determined using

$$\alpha = 0.15v + 2.14 \quad (10)$$

Where v represents the wind speed given in m/s.

Even though Fig. 4 shows the relationship between the wind speed and the environmental parameter α , there seems to be a significant discrepancy at medium wind speeds. This may indicate that either there are other factors that need to be taken into account, or that a larger data set is needed for a statistically proper development of the model.

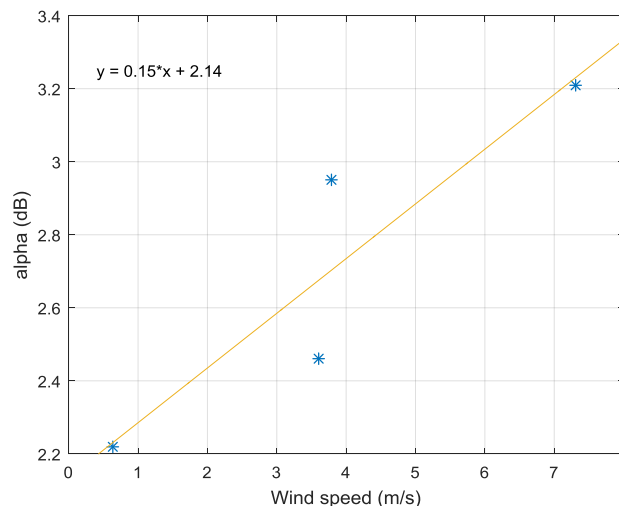


Figure 4. Relationship between parameter α and wind speed

V. MODEL EVALUATION

The model described in (1)-(10) is tested on all the data collected during the four experiments. The results of the model prediction are shown in Fig. 5. Also, Table 6 characterizes the prediction error. To determine the mean and standard deviation of the error, all collected data from Tables 2, 4, 6 and 8 in

[6] are used. As seen, there is a good agreement between the measurements and predictions. The average prediction error is close to zero with standard deviation of the error on the order of 3-4dB, except for experiment E-3. This may be considered adequate for network planning purposes, as it leads to reasonable fade margin values [9].

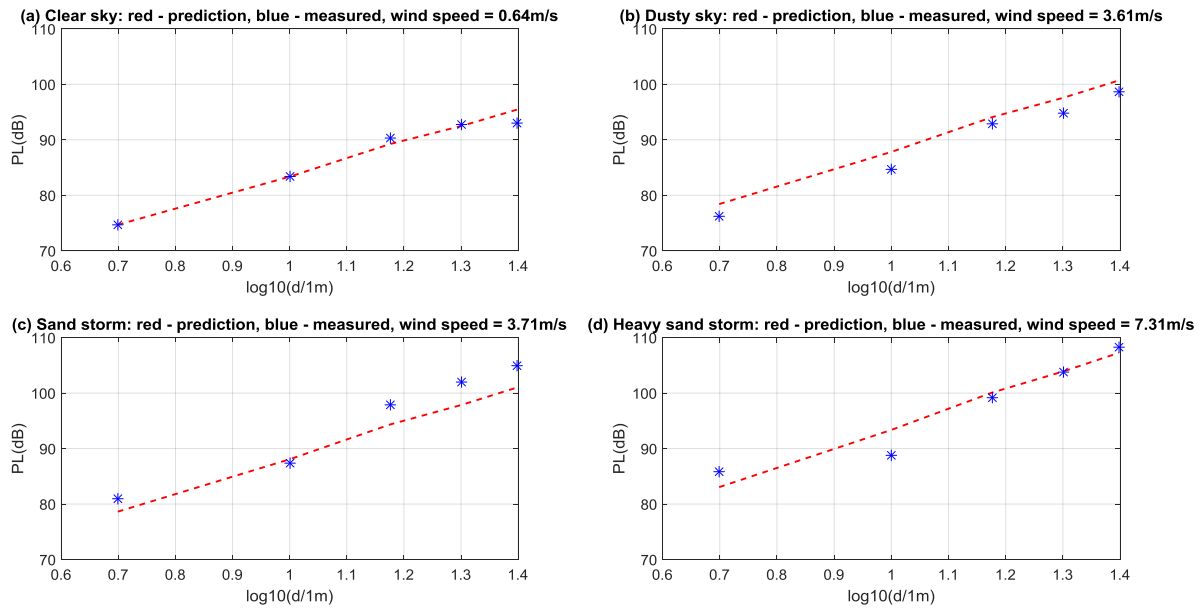


Figure 5. Comparison between the model predictions and measured data

TABLE 6. Evaluation of the prediction error

Environment	Mean error (dB)	Standard deviation (dB)
E1 – clear sky	-0.2	3.2
E2 – dusty sky	-2.2	7.1
E3 – sand storm	2.6	3.5
E4 – heavy sand storm	-0.3	3.1

VI. CONCLUSION AND FUTURE WORK

This paper presents an empirical model for WSN operating in sand storm environment. The model is based on data collected in 2.4GHz ISM band which is one of the most popular WSN bands. The model may be seen as a generalization of the two-ray propagation where a term is added to take into account the absorption of the radio wave that is due to presence of sand and dust particles. Furthermore, it is revealed that the wind speed is the most significant factor impacting the level of the additional attenuation. Except in one of the conducted experiments, the mean of the prediction error is smaller than 2.2dB, with standard deviation on the order 3-4dB. Even in the worst case scenario the standard deviation of the prediction error is on the order 7dB, which allows for a reasonable planning of the network.

Some follow up to this work would be appropriate. First, there is an obvious need for a more empirical thorough model verification. Also, the severity of the storm may need additional characterization in terms of influencing factors. Based on the findings in this paper, the wind speed seems to be significant, but not the only factor. Finally, the form of the factor used by the model to

capture additional losses due to sand and dust was determined through trial and error. Some physical insight and justification of this factor is highly desirable.

REFERENCES

- [1]. P. Z. Wang, M. Vuran, M. Al-Rodhaan, A. Al-Dhelaan and I. Akyildiz, "Topology Analysis of Wireless Sensor Networks for Sandstorm Monitoring," in *Communications (ICC), 2011 IEEE International Conference*, Atlanta, 2011.
- [2]. E. M. Abuhdima and I. M. Saleh, "Effecs of sand and dust storms on microwave propagation in southern Libya," *15th IEEE Mediterranean Electrotechnical Conference*, Valletta, 2010.
- [3]. S. Ghabrial, and D. Sharif, "Microwave Attenuation and Cross Polarization in Dust Storms," *IEEE Transactions on Antennas and Propagation*, Vol. AP-35, No 4.
- [4]. G. Comparetto, "The Impact of Dust and Foliage on Signal Attenuation in the Millimeter Wave Regime," Originally published in *J. of Space Communications*, Vol 11, no. 1, pp.13-20, Jul 1993.

- [5]. A. AlSayyari, I. Kostanic, C. Otero, M. Almeer and K. Rukieh, "An empirical path loss model for wireless sensor network deployment in a sand terrain environment," in *Internet of Things (WF-IoT), 2014 IEEE World Forum on*, Seoul, Korea, 2014.
- [6]. H. Mijlid and I. Kostanic, "Propagation Path Loss Measurements for Wireless Sensor Networks in Sand and Dust Storms," In (Frontiers in Sensors (FS) - Science and Engineering Publishing Company) accepted.
- [7]. J. D. Parsons, *Mobile Radio Propagation Channel*, 2nd edition, John Wiley & Sons, 2000.
- [8]. -, ITU Report P.1008-1 (1990), *Reflection from the surface of the Earth*.
- [9]. W. Jakes, *Microwave Mobile Communications (An IEEE Press Classic Reissue)*, Wiley-IEEE Press; 2nd edition (May 16, 1994).

Hana Mujlid, et. al. "Empirical Path Loss Prediction for Wireless Sensor Networks Operating in Sand and Dust Storms." *International Journal of Engineering Research and Applications (IJERA)*, vol.11 (1), 2021, pp 25-32.